Synthesis and characterization of non-stoichiometric hydroxyapatite nanoparticles using unmodified and modified starches

Síntese e caracterização de nanopartículas de hidroxiapatita não estequiométrica usando amidos não modificados e modificados

Síntesis y caracterización de nanopartículas de hidroxiapatita no estequiométricas utilizando almidones sin modificar y modificados

Geraldine Nancy Rodriguez Perea

ORCID: https://orcid.org/0000-0002-9013-340X

Universidade Federal Fluminense, Brazil

E-mail: geraldineperea@id.uff.br

Mariana Bianchini Silva

ORCID: https://orcid.org/0000-0002-3207-9687

Universidade Federal Fluminense, Brazil

E-mail: marianabianchini@id.uff.br

Bruno Xavier Freitas

ORCID: https://orcid.org/0000-0001-7721-7687

Universidade de São Paulo, Brazil

E-mail: bxfreitas@hotmail.com

Ésoly Madeleine Bento dos Santos

ORCID: https://orcid.org/0000-0002-0940-0540

Universidade Federal Fluminense, Brazil

E-mail: esolysantos@id.uff.br

Luiz Carlos Rolim Lopes

ORCID: https://orcid.org/0000-0002-6298-2447

Universidade Federal Fluminense, Brazil

E-mail: luiz.crolim@uol.com.br

Letícia Vitorazi

ORCID: http://orcid.org/0000-0002-6626-9016

Universidade Federal Fluminense, Brazil

E-mail: leticiavitorazi@id.uff.br

Claudinei dos Santos

ORCID: https://orcid.org/0000-0002-9398-0639

Universidade do Estado do Rio de Janeiro, Brazil

E-mail: claudineisvr@gmail.com

Abstract

Non-stoichiometric hydroxyapatite (HAp) presents an additional phase in its structure due to calcium or phosphorus excess, which can influence the material's mechanical properties, as well as its bioactivity and biodegradability. While stoichiometric HAp, with calcium to phosphorus ratio (Ca/P) of 1.67, has been widely investigated, only a few studies have reported the synthesis of HAp with higher Ca/P ratio. In this work, non-stoichiometric HAp nanoparticles were synthesized using chemical precipitation method followed by a calcination protocol. In order to achieve better process control with chemical precipitation, starch, a natural additive, was applied. Three types of starch were selected for comparison: nonionic starch (NS), soluble starch (SS), and cationic starch (CS). Infrared spectroscopy and chemical analysis results confirmed the non-stoichiometric profile of the synthesized HAp, with a 1.98 Ca/P ratio. X-ray diffraction (XRD) results showed that HAp and calcium oxide (CaO) crystalline phases were obtained and no residual starch was detected. Rietveld refinements confirmed that, for all three types of starch, the content of crystalline HAp was greater than 96.5% and the unit cell volume was not affected. Scanning electron microscopy (SEM) showed agglomeration of particles. Nanoparticle tracking analysis (NTA) results demonstrated that the use of SS produced the smallest particles (approximately 60nm).

Keywords: Nanopowder; Chemical precipitation; Calcium-rich hydroxyapatite; Calcium oxide.

Resumo

A hidroxiapatita (HAp) não estequiométrica apresenta uma fase adicional em sua estrutura devido ao excesso de cálcio ou fósforo que pode influenciar nas propriedades mecânicas do material, assim como sua bioatividade e biodegradabilidade. Embora a HAp estequiométrica, com um valor de razão cálcio/fósforo (razão Ca/P) de 1.67, tenha sido amplamente investigada, apenas alguns estudos reportaram a síntese de HAp com uma razão Ca/P mais alta que o valor estequiométrico. Neste trabalho, nanopartículas de HAp não estequiométrica foram sintetizadas usando o método de precipitação química seguida de um protocolo de calcinação. Para um melhor controle do processo por precipitação química, amido, um aditivo

natural, foi adicionado ao processo. Três tipos de amido foram selecionados para comparação: amido não iônico (NS), amido solúvel (SS) e amido catiônico (CS). Os resultados de espectroscopia no infravermelho e a análise química confirmaram o perfil não estequiométrico da HAp sintetizada, com uma razão Ca/P de 1.98. Os resultados de difração de raios X (DRX) mostraram que foram obtidas fases cristalinas de HAp e de óxido de cálcio (CaO) e nenhum amido residual foi detectado. Os refinamentos de Rietveld confirmaram que, para os três tipos de amido, o conteúdo de HAp cristalina foi superior a 96,5% e o volume da célula unitária não foi afetado. A microscopia eletrônica de varredura (MEV) mostrou aglomeração de partículas. Os resultados da análise de rastreamento de nanopartículas (NTA) demonstraram que o uso de SS produziu as menores partículas (aproximadamente 60 nm).

Palavras-chave: Nanopó; Precipitação química; Hidroxiapatita rica em cálcio; Óxido de cálcio.

Resumen

La hidroxiapatita (HAp) no estequiométrica presenta una fase adicional en su estructura debido al exceso de calcio o fósforo, que puede influir en las propiedades mecánicas del material, como em su bioactividad y biodegradabilidad. Aunque la HAp estequiométrica, con un valor de relación calcio/fósforo (Ca/P) de 1,67 se ha investigado ampliamente, solo unos pocos estudios han informado síntesis de HAp con una relación de Ca/P más alta que o valor estequiométrico. En este trabajo, nanopartículas de HAp no estequiométricas fueron sintetizadas utilizando el método de precipitación química seguido de un protocolo de calcinación. Para un mejor control del proceso por precipitación química, almidón, un aditivo natural, fue agregado al processo. Se seleccionaron tres tipos de almidón para ser comparados: almidón no iónico (NS), almidón soluble (SS) y almidón catiónico (CS). La espectroscopia infrarroja y el análisis químico confirmaron el perfil no estequiométrico de la HAp sintetizada, con una relación Ca/P de 1,98. Los resultados de difracción de rayos X (DRX) mostraron que se obtuvieron fases cristalinas de HAp y óxido de calcio (CaO) y no se detectó almidón residual. Los refinamientos de Rietveld confirmaron que, para los tres tipos de almidón, el contenido de HAp cristalina fue superior al 96,5% y el volumen de la celda unitaria no se vio afectado. La microscopía electrónica de barrido (MEB) mostró aglomeración de partículas. Los resultados del análisis de seguimiento de nanopartículas (NTA) demostraron que el uso de SS produjo las partículas más pequeñas (aproximadamente 60 nm).

Palabras clave: Nanopolvos; Precipitación química; Hidroxiapatita rica en cálcio; Óxido de cálcio.

1. Introduction

The synthesis of stoichiometric hydroxyapatite (HAp) has been widely studied for decades (Araújo et al., 2020; Bonel et al., 1988; Brown et al., 1991; Greish, 2011; Kakiage et al., 2015), but only a few authors have reported results on the synthesis of calcium-rich HAp sintering or characteristics of HAp and CaO (Bengtsson et al., 2009; Kim et al., 2005; Omori et al., 2014; Raynaud et al., 2002).

Differences in mechanical proprieties, bioactivity and biodegradability are a result of variation in Ca/P ratio in the HAp structure. These differences are related to the presence of a second phase within the material, especially calcium triphosphate (TCP) in HAp with Ca/P ratio below 1.67 and calcium oxide (CaO) when Ca/P ratio is higher than 1.67 (Ramesh et al., 2007; Ravaglioli & Krajewski, 1992), while at stoichiometric ratio these phases aren't observed. Some authors have observed that the presence of CaO in HAp can reduce the material's flexural strength, possibly because stoichiometric HAp presents densification around 99% while non-stoichiometric HAp presents a 97% densification degree after sinterization (Ramesh et al., 2007; Royer et al., 1993). Regardless of the negative effect over its mechanical proprieties, non-stoichiometric HAp can be considered satisfactory for some applications because both CaO and TCP are more soluble in water than pure HAp, thus benefiting the material's biodegradability. The CaO presence stimulates bone formation as the excess of calcium ions promotes HAp nucleation (Kim et al., 2005; Wang et al., 2003). Also, when synthesizing HAp nanoparticles, CaO formed around the particles may be interesting to prevent nanoparticles aggregation (Kakiage et al., 2015; Okada & Furuzono, 2007).

The most commonly used method to prepare HAp is the chemical precipitation method due to its simplicity and low cost (Gomes et al., 2020). A disadvantage of this method, however, is the production of unwanted crystalline phases and low crystallinity of the powders (Yang et al., 2013). Organic additives can be introduced to the synthesis protocol to induce anisotropic growth of the crystal faces after initial nucleation by face-selective adsorption of the additive (Meskinfam, 2011; Sadat-Shojai et al., 2013). An alternative for better process control is the use of additives and/or modifiers in the conventional process, such as cetyl trimethyl ammonium bromide, polyvinylpyrrolidone, and polyethylene glycol. However, the use of these surfactants has raised concern due to controversial results regarding

toxicity and biocompatibility. In this context, the use of natural additives such as corn starch is promising to produce biocompatible HAp nanoparticles (Masina et al., 2017; Small, 1919; Yang et al., 2013). Water-soluble starch can be used in HAp synthesis because its characteristics facilitate strong adhesion between the HAp and starch (Miculescu et al., 2017). Starch is a natural biopolymer, biodegradable, biocompatible, water-soluble and inexpensive in comparison to other biodegradable polymers (Jane, 2015; Motta et al., 2020; Sadjadi et al., 2010) and seems to be a good candidate as an additive to produce HAp nanoparticle.

Starch consists of amylose and amylopectin in different percentages, varying according to its botanical source (Jane, 2015; Omori et al., 2014). Starch has several applications in bioceramics synthesis: it can reduce agglomeration, act as a control agent of pore-forming, and improve biological and mechanical properties (Mastalska-Poplawska et al., 2019). Different types of starch (corn, crosslinked, cationic, and calcium-modified) were used by Liu *et al.* to improve the properties of cement-based calcium phosphates (Liu et al., 2016; Miculescu et al., 2017). Nonionic starch is already widely used to obtain nanocrystalline HAp powders (Meskinfam, 2011; Sadjadi et al., 2010); however, starch modifications can be produced in order to change its physical-chemical and mechanical properties (Jane, 2015; Omori et al., 2014). Cationic starches, for example, are obtained from the reaction with a cationic agent that promotes a physical-chemical transformation responsible for enhanced viscosity and lower gelatinization temperatures (Motta et al., 2020). Soluble starches present high solubility in hot water and can be produced by enzymatic action, acid hydrolysis, or by superheated steam (Small, 1919).

In this work, HAp nanoparticles were synthesized and characterized using starch as an additive. To compare the effect of different types of starch over the synthesis process and the final material, three samples of HAp powders were prepared using nonionic (NS), soluble (SS) and cationic (CS) starches.

2. Experimental Procedure

Calcium nitrate tetrahydrate (Ca(NO$_3$)$_2$.4H$_2$O; Synth; P.A.) and phosphoric acid solution (H$_3$PO$_4$-85%; Synth; P.A.) were used as precursor materials for HAp synthesis, with ammonium hydroxide (NH$_4$OH, Synth; P.A.) as a precipitation agent. Nonionic starch (Santi Indústria, Brazil), soluble starch (Proquímios; P.A.) and cationic starch (FOXHEAD5804, Ingredion) were used to prepare the pre-nucleation solutions.

The synthesis protocol was based on Lima *et al.* (Lima et al., 2017) work with

modifications. A pre-nucleation solution was prepared with nonionic starch (4g) and $Ca(NO_3)_2.4H_2O$ (Ca 39.4g; 0.167 mol) in water (96g) and heated at 90ºC for 40min under magnetic stirring to promote starch gelatinization. To the pre-nucleation solution under stirring and at room temperature, 100g of H_3PO_4 aqueous solution (P; 0.085 mol) at 8.3wt.% were added dropwise to achieve non-stoichiometric ratio Ca/P (in mol)=1.98. The pH of the mixture was adjusted from 1to10 by NH_4OH addition, resulting in a viscous mixture with precipitate. The removal of solvents or supernatant in a drying oven at 100ºC for 72h yielded a raw yellowish material that was pre-calcined at 300ºC for 2h and calcined at 700ºC for 4h in a muffle furnace. After each pre-calcination and calcination process, the particle size was reduced by crushing in an agate mortar. The final product was a white powder. The same preparation protocol used for NS was applied in the syntheses using SS and CS with the difference that for CS the gelatinization temperature applied was 80ºC.

A chemical analysis was performed by inductively coupled plasma with optical emission spectroscopy (ICP-OES) to determine the Ca/P molar ratio. A small amount of each powder sample (0,1g) was digested in concentrated nitric acid, then diluted with distilled water. The samples were analyzed with a Shimadzu atomic emission spectrophotometer (ICP 9000).

An absorption spectrophotometer was used in the infrared region under attenuated total reflectance (ATR) (model FT/IR-4700, Jasco Corporation, Japan) in transmittance, between 400 and 3500 cm^{-1}, using 32 scans at a resolution of 4 cm^{-1}.

X-ray diffraction of HAp powders was performed using Panalytical equipment, Ni-filtered Cu(kα) radiation (λ=1.5418Å), with an exposure time of 3s/point and step of 0.02°. Phase identification and Rietveld refinements from XRD data were performed using the FullProf software (Rodríguez-Carvajal, 1993). The crystallographic data from COD 9013627 and ICSD 261847 for HAp and CaO phases, respectively, proved the obtainment of the two compounds. The peak profiles modeled by Pseudo-Voigt function with background fitted by 6-coefficients polynomial function refined the parameters as scale factor, unit cell, background, Full width at half maximum parameter (FWHM), instrumental zero, and atoms positions. FWHM parameters gave the crystalline size of the powders by application of Scherrer's equation.

Morphology of the HAp powder was investigated with scanning electron microscopy (SEM): around 10uL of a HAp aqueous dispersion (1wt.%) dripped onto a surface of a carbon tape fixed at SEM sample holder previously dried in a desiccator. Acquired images used the secondary electron detector (Jeol JSM-5800LV) with parameters of 12kV voltage and 12mm

of working distance.

The HAp particles were dispersed in isopropyl alcohol (1wt%) and analyzed by Nanoparticle Tracking Analysis (NTA-Malvern Panalytical). 60 seconds videos were recorded for each sample at 25ºC with a red laser application (635 nm), estimating a range of 10-40 particles per image, and the data collected were processed with NTA2.3 Analytical software.

3. Results and Discussion

Hydroxyapatite is a ceramic material which applicability can be defined by its chemical stoichiometry. The Ca/P molar ratio obtained for each sample is presented in Table 1. For all samples, the HAp obtained was non-stochiometric (with Ca/P ratio higher than the stoichiometric value, 1.67), although there was no relevant difference among the different starches used.

Table 1. Ca/P molar ratio of synthesized HAp powders according to the type of starch applied. The amount of Ca and P present in each sample was obtained by trace chemical analysis.

Sample	Ca/P molar ratio
NS	1.93
SS	1.92
CS	1.95

Source: Authors.

The obtained infrared spectra, presented in Figure 1, were similar for all synthesized samples and indicate incorporation of HPO_4^{2-} groups in the crystalline lattice, rather than PO_4^{3-} groups. Table 2 presents the most significant bands observed in the FTIR spectra with their respective assigned groups. Bands located around 470, 570, 600 and 1050 cm^{-1} were assigned to PO_4^{3-} group, while the band located around 875 cm^{-1} is attributed to HPO_4^{2-} (Fowler, 1974; Meskinfam, 2011; Omori et al., 2014; Rey et al., 2017), and the band at 1420 cm^{-1} can be attributed to CO_3^{2-} substituted phosphate positions in the HAp lattice (Omori et al., 2014). These observed FTIR peaks suggest the chemical formula $Ca_{10-x}(PO_4)_{6-x}(HPO_4)_x(OH)_{2-x}$ for the synthesized HAp (Ishikawa et al., 1993).

Figure 1. FTIR spectra of synthesized HAp powders for different types of starch. Relevant bands were similar for all analyzed samples, indicating similar structures were obtained.
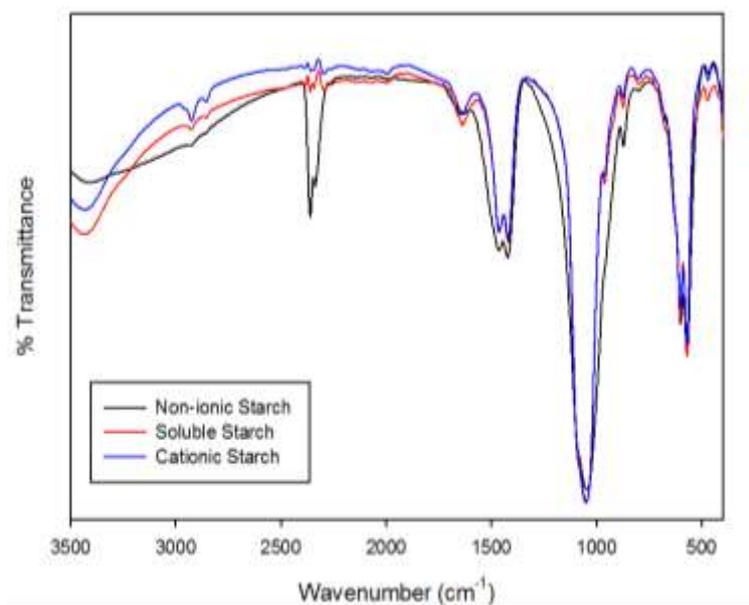
Source: Authors.

Table 2. Assignments of relevant FTIR bands obtained for synthesized HAp powders.

Band wavenumber			Band assignment
NS (cm⁻¹)	SS (cm⁻¹)	CS (cm⁻¹)	
3402	3430	3432	O-H stretching
1463	1464	1464	CO_3^- groups
1423	1420	1421	C-O υ stretching mode
1046	1050	1051	P-O υ_3 stretching mode - PO_4^{3-}
873	875	874	P-O bond - HPO_4^{2-}
602	603	603	O-P-O υ_4 bending mode - PO_4^{3-}
570	571	571	O-P-O υ_4 bending mode - PO_4^{3-}
470	472	472	O-P-O υ_2 bending mode - PO_4^{3-}

Source: Authors.

Figure 2 shows XRD patterns of synthesized HAp and Table 3 presents Rietveld refinements results obtained about the three studied powders. These results indicate the presence of HAp and residual CaO as nanocrystalline phases. Under all synthetic conditions used in this work, the content of crystalline HAp evaluated by Rietveld refinement was

greater than 96.5%. Furthermore, no residual starch appeared in the powders, which indicates that after calcination all organic content was eliminated (Lima et al., 2017).

Figure 2. XRD patterns of HAp and CaO and synthesized HAp powders for comparison.
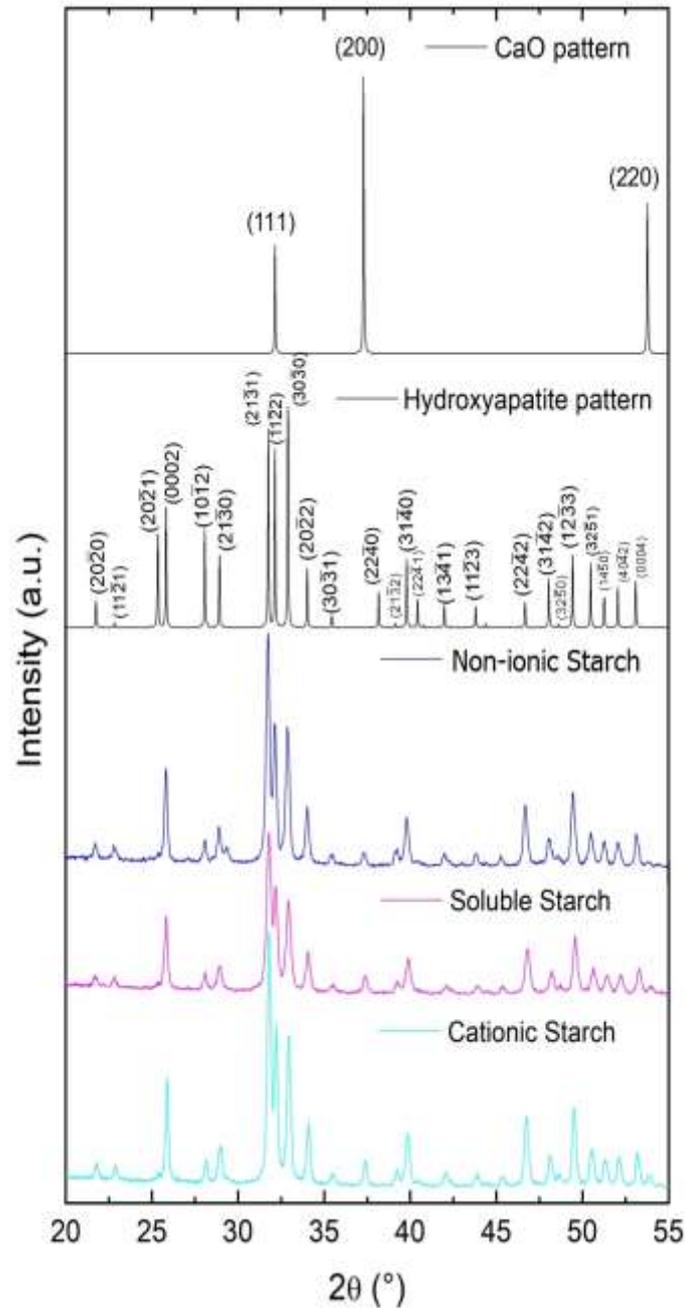
Source: Authors.

Table 3. Rietveld refinement of crystalline phases in synthesized HAp powders with calculated lattice parameters and cell volume for Hap and CaO phase, as well as the mass percentage of each phase.

| Starch | Hap [24] – Space Group (176) | | CaO [25] – Space Group (225) | | wt. % phase Hap/CaO | Crystallite size (nm) | Rp | Rwp | Re | χ^2 |
	Lattice parameters (nm)	Cell volume (nm³)	Lattice parameters (nm)	Cell volume (nm³)						
Non-ionic	a=b=0.941(4) c=0.688(3)	0.5282	a=b=c=0.481(1)	0.1113	97.7/2.3	**40**	14.2	18.0	14.6	**1.5**
Soluble	a=b=0.941(3) c=0.688(5)	0.5283	a=b=c=0.481(1)	0.1113	96.7/3.3	**35**	13.9	16.5	15.9	**1.1**
Cationic	a=b=0.941(7) c=0.688(5)	0.5287	a=b=c=0.481(2)	0.1114	96.5/3.5	**35**	11.9	14.8	13.7	**1.2**

Source: Authors.

The refined crystalline parameters from the diffractogram (Table 3) indicate that the net parameters are similar for all synthesized HAp (a = b = 0.941 nm and c = 0.688nm), and, consequently, the unit cell volume was not affected by the type of starch used in synthesis. Similar results were observed for CaO, where the net parameter is 0.481nm. The χ^2 values, varying from 1.1 to 1.5, demonstrate the quality of the Rietveld refinement. The nanocrystalline domains of the synthesized powders are shown by the crystallite sizes calculated with values between 35 and 40 nm.

Usually, studies about synthetic HAp apply a 1.67 ratio between Ca and P, corresponding to the formation reaction of stoichiometric hydroxyapatite $Ca_{10}(PO_4)_6(OH)_2$. In this study, a 1.98 Ca/P ratio was used and the excess of calcium justifies the formation of residual CaO phase. The amount of CaO obtained was about 2.3 – 3.5 %, corresponding to the 16 % excess of calcium added to the formation reaction.

Figure 3 presents the SEM micrographs, showing the morphological aspects of the different powders. For all analyzed powders, agglomerates of non-regular particles were observed. Note that the agglomeration degree doesn't allow a detailed size and morphology analysis of individualized particles and therefore does not allow the identification of nanometric characteristics in the materials via SEM. Thus, these three powders were analyzed using a particle analyzer associated with crystallographic characterizations.

Figure 3. SEM micrographs of synthesized HAp powders, with agglomerated particles that required further size characterization: (a) NS, (b) SS and (c) CS at 2000x magnification.

(a)　　　　　　　　　　(b)　　　　　　　　　　(c)
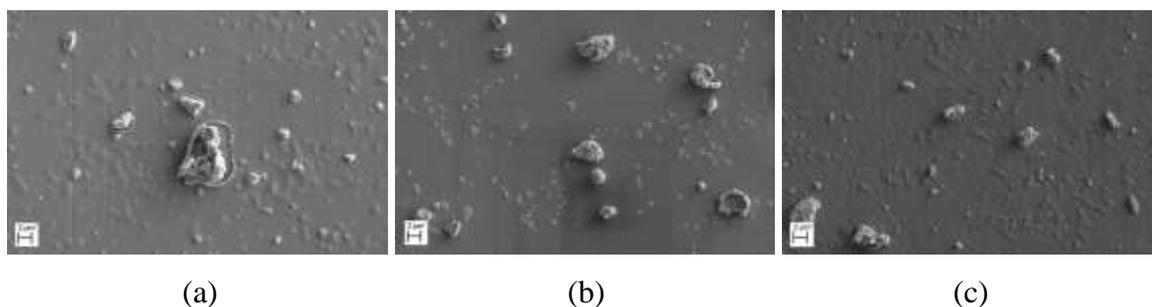
Source: Authors.

The particle-size distributions for the HAp dispersions were registered using nanoparticle tracking analysis (Figure 4a) and the average diameters of HAp particles obtained from different starches were calculated (Figure 4b). A particle size distribution curve represents the number of particles identified for each scanned size in terms of particle concentration. Curves for all studied systems presented one peak (monomodal), regardless of the type of starch used, indicating a monodisperse material. The synthesis using SS produced the smallest particles, with an average diameter of 60nm, and a narrow size distribution curve. The use of CS and NS yields bigger HAp particles, with 87nm and 105nm, respectively, and broader particle size distributions.

Figure 4. Investigation of particle sizes for each sample performed by NTA. (a) Particle size distribution curves obtained and (b) Calculated average particle size (with standard deviation indicated for each sample) of synthesized HAp powders.

(a)　　　　　　　　　　　　　　　　　(b)
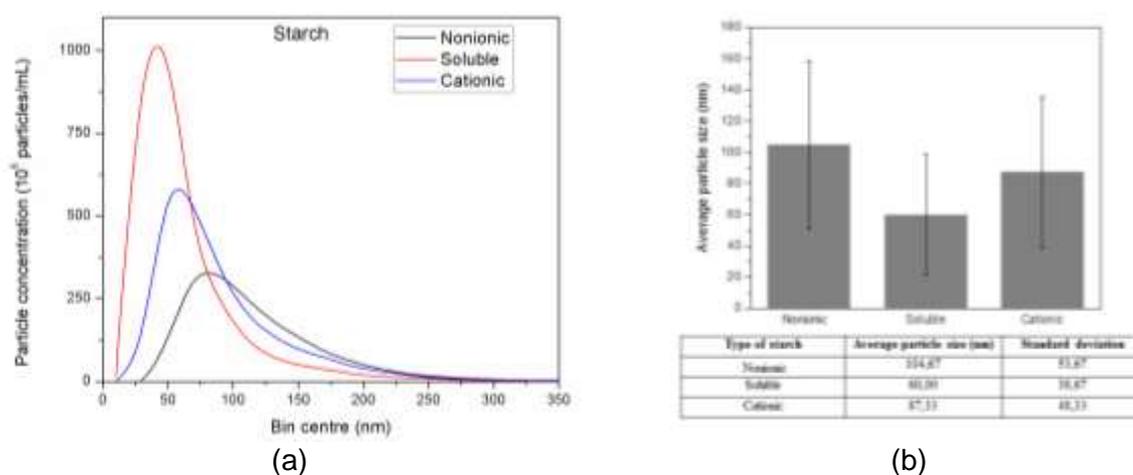
Source: Authors.

Nonmodified starches (NS and SS) present the highest gelatinization temperature

(90ºC) (Motta et al., 2020) and the amylopectin in its composition is associated with the crystallinity of the granules (Jane, 2015). The main limitation of using soluble starch is its high degree of purity, increasing production cost (Nawaz et al., 2020). Usually, modified starches containing cationic and anionic groups are less sensitive for retrogradation and syneresis (Kaur & Singh, 2016) which makes them useful in the industry. Thus, one can achieve gelation temperature more easily and decrease retrogradation and syneresis process when using modified starches.

4. Conclusions

The high percentage of HAp crystalline phase observed in the synthesized material demonstrated that the method investigated, which used starch as an additive, was a valid synthetic route. CaO phase in the non-stoichiometric HAp makes it more susceptible to degradation, benefiting its application as a biomaterial.

Although SEM micrographs exhibited agglomerated particles with irregular-shape morphology, different crystallite and particle sizes, within the nanometer scale, were obtained for HAp powders synthesized with the three types of starches.

All three types of starch added in synthesis led to nanosized HAp particles, with no difference relevance when comparing the results and considering the standard error.

In order to continue the work, we suggest homogenization and deglomeration of particles within the hydroxyapatite powders using the ball mill and characterization regarding the particles' size and morphology.

Acknowledgments

References

Araújo, M. N. P., Vieira, W. E. da S., Carvalho, L. P. de, Melo, H. D. F. de, Souza, T. C. de, & Berenguer, R. A. (2020). Obtenção e caracterização de hidroxiapatita obtida por síntese hidrotermal e caracterização. *Research, Society and Development*, *9*(11), e535911100247–e535911100247.

Bengtsson, Å., Shchukarev, A., Persson, P., & Sjöberg, S. (2009). A solubility and surface complexation study of a non-stoichiometric hydroxyapatite. *Geochimica et Cosmochimica Acta*, *73*(2), 257–267.

Bonel, G., Heughebaert, J.-C., Heughebaert, M., Lacout, J. L., & Lebugle, A. (1988). Apatitic Calcium Orthophosphates and Related Compounds for Biomaterials Preparation. *Annals of the New York Academy of Sciences*, *523*(1 Bioceramics), 115–130.

Brown, P. W., Hocker, N., & Hoyle, S. (1991). Variations in Solution Chemistry During the Low-Temperature Formation of Hydroxyapatite. *Journal of the American Ceramic Society*, *74*(8), 1848–1854.

Fowler, B. O. (1974). Infrared studies of apatites. I. Vibrational assignments for calcium, strontium, and barium hydroxyapatites utilizing isotopic substitution. *Inorganic Chemistry*, *13*(1), 194–207.

Gomes, F. D. C., Amorim, J. D. P. de, Silva, G. S. da, Souza, K. C. de, Pinto, A. F., Santos, B. S., & Costa, A. F. de S. (2020). Preparation and Characterization of Hydroxyapatite by the precipitation method and heat treatment. Research, Society and Development, 9(6), e172963549–e172963549.

Greish, Y. E. (2011). Phase evolution during the low temperature formation of stoichiometric hydroxyapatite-gypsum composites. *Ceramics International*, *37*(3), 715–723.

Ishikawa, K., Ducheyne, P., & Radin, S. (1993). Determination of the Ca/P ratio in calcium-deficient hydroxyapatite using X-ray diffraction analysis. *Journal of Materials Science: Materials in Medicine*, *4*(2), 165–168.

Jane, J. (2015). Starch Properties, Modifications, and Applications. *Journal of Macromolecular Science, Part A*, *52*(12), ebi-ebi.

Kakiage, M., Iwase, K., & Kobayashi, H. (2015). Effect of citric acid addition on disaggregation of crystalline hydroxyapatite nanoparticles under calcium-rich conditions. *Materials Letters*, *156*, 39–41.

Kaur, L., & Singh, J. (2016). Starch: Modified Starches. In *Encyclopedia of Food and Health* (pp. 152–159). Elsevier.

Kim, S., Ryu, H.-S., Shin, H., Jung, H. S., & Hong, K. S. (2005). In situ observation of hydroxyapatite nanocrystal formation from amorphous calcium phosphate in calcium-rich solutions. *Materials Chemistry and Physics*, *91*(2–3), 500–506.

Lima, T. A. R. M., Ilavsky, J., Hammons, J., Sarmento, V. H. V., Rey, J. F. Q., & Valerio, M. E. G. (2017). Synthesis and synchrotron characterisation of novel dual-template of hydroxyapatite scaffolds with controlled size porous distribution. *Materials Letters*, *190*, 107–110.

Liu, H., Guan, Y., Wei, D., Gao, C., Yang, H., & Yang, L. (2016). Reinforcement of injectable calcium phosphate cement by gelatinized starches. *Journal of Biomedical Materials Research Part B: Applied Biomaterials*, *104*(3), 615–625.

Masina, N., Choonara, Y. E., Kumar, P., Toit, L. C. du, Govender, M., Indermun, S., & Pillay, V. (2017). A review of the chemical modification techniques of starch. *Carbohydrate Polymers*, *157*, 1226–1236.

Mastalska-Poplawska, J., Sikora, M., Izak, P., & Goral, Z. (2019). Applications of starch and its derivatives in bioceramics. *Journal Of Biomaterials Applications*, *34*(1), 12–24.

Meskinfam, M., M. A. S|Jazdarreh, H|Zare, K. (2011). Biocompatibility evaluation of nano hydroxyapatite-starch biocomposites. *Journal of Biomedical Nanotechnology*, *7*(3), 455–459.

Miculescu, F., Maidaniuc, A., Voicu, S. I., Thakur, V. K., Stan, G. E., & Ciocan, L. T. (2017). Progress in Hydroxyapatite–Starch Based Sustainable Biomaterials for Biomedical Bone Substitution Applications. *ACS Sustainable Chemistry & Engineering*, *5*(10), 8491–8512.

Motta, J. F. G., de Souza, A. R., Gonçalves, S. M., Madella, D. K. S. F., de Carvalho, C. W. P., Vitorazi, L., & de Melo, N. R. (2020). Development of active films based on modified starches incorporating the antimicrobial agent lauroyl arginate (LAE) for the food industry. *Food and Bioprocess Technology*.

Nawaz, H., Waheed, R., Nawaz, M., & Shahwar, D. (2020). Physical and Chemical Modifications in Starch Structure and Reactivity. In M. Emeje (Ed.), *Chemical Properties of Starch*. IntechOpen.

Okada, M., & Furuzono, T. (2007). Nano-Sized Ceramic Particles of Hydroxyapatite Calcined with an Anti-Sintering Agent. *Journal of Nanoscience and Nanotechnology*, *7*(3), 848–851.

Omori, Y., Okada, M., Takeda, S., & Matsumoto, N. (2014). Fabrication of dispersible calcium phosphate nanocrystals via a modified Pechini method under non-stoichiometric conditions. *Materials Science and Engineering: C*, *42*, 562–568.

Ramesh, S., Tan, C. Y., Hamdi, M., Sopyan, I., & Teng, W. D. (2007). *The influence of Ca/P ratio on the properties of hydroxyapatite bioceramics*. 64233A.

Ravaglioli, A., & Krajewski, A. (1992). *Bioceramics*. Springer Netherlands.

Raynaud, S., Champion, E., Bernache-Assollant, D., & Thomas, P. (2002). Calcium phosphate apatites with variable Ca/P atomic ratio I. Synthesis, characterisation and thermal stability of powders. *Biomaterials*, *23*(4), 1065–1072.

Rey, C., Combes, C., Drouet, C., Grossin, D., Bertrand, G., & Soulié, J. (2017). 1.11 Bioactive Calcium Phosphate Compounds: Physical Chemistry ☆. In *Comprehensive Biomaterials II* 244–290).

Rodríguez-Carvajal, J. (1993). Recent advances in magnetic structure determination by neutron powder diffraction. *Physica B: Condensed Matter*, *192*(1–2), 55–69.

Royer, A., Viguie, J. C., Heughebaert, M., & Heughebaert, J. C. (1993). Stoichiometry of hydroxyapatite: Influence on the flexural strength. *Journal of Materials Science: Materials in Medicine*, *4*(1), 76–82.

Sadat-Shojai, M., Khorasani, M.-T., Dinpanah-Khoshdargi, E., & Jamshidi, A. (2013). Synthesis methods for nanosized hydroxyapatite with diverse structures. *Acta Biomaterialia*, *9*(8), 7591–7621.

Sadjadi, M. S., Meskinfam, M., Sadeghi, B., Jazdarreh, H., & Zare, K. (2010). In situ biomimetic synthesis, characterization and in vitro investigation of bone-like nanohydroxyapatite in starch matrix. *Materials Chemistry and Physics*, *124*(1), 217–222.

Small, J. C. (1919). A method for the preparation of soluble starch. *Journal of the American Chemical Society*, *41*(1), 113–120.

Wang, H., Lee, J.-K., Moursi, A., & Lannutti, J. J. (2003). Ca/P ratio effects on the degradation of hydroxyapatitein vitro. *Journal of Biomedical Materials Research*, *67* (2), 599–608.

Yang, L., Ning, X., Bai, Y., & Jia, W. (2013). A scalable synthesis of non-agglomerated and low-aspect ratio hydroxyapatite nanocrystals using gelatinized starch matrix. *Materials Letters*, *113*, 142–145.

Percentage of contribution of each author in manuscript

Geraldine Nancy Rodriguez Perea – 20%

Mariana Bianchini Silva – 15%

Bruno Xavier Freitas – 10%

Ésoly Madeleine Bento dos Santos – 15%

Luiz Carlos Rolim Lopes – 10%

Letícia Vitorazi – 15%

Claudinei dos Santos – 15%